Production and evolution of perturbations of sterile neutrino dark matter

Kevork Abazajian

Theoretical Division, Los Alamos National Laboratory, MS B285, Los Alamos, New Mexico 87545, USA

(Received 22 November 2005; published 10 March 2006)

Sterile neutrinos, fermions with no standard model couplings [SU(2) singlets], are predicted by most extensions of the standard model, and may be the dark matter. I describe the nonthermal production and linear perturbation evolution in the early universe of this dark matter candidate. I calculate production of sterile neutrino dark matter including effects of Friedmann dynamics dictated by the quark-hadron transition and particle population, the alteration of finite temperature effective mass of active neutrinos due to the presence of thermal leptons, and heating of the coupled species due to the disappearance of degrees of freedom in the plasma. These effects leave the sterile neutrinos with a nontrivial momentum distribution. I also calculate the evolution of sterile neutrino density perturbations in the early universe through the linear regime and provide a fitting function form for the transfer function describing the suppression of small-scale fluctuations for this warm dark matter candidate. The results presented here differ quantitatively from previous work due to the inclusion of the relevant physical effects during the production epoch.

DOI: 10.1103/PhysRevD.73.063506 PACS numbers: 95.35.+d, 14.60.Pq, 14.60.St, 98.65.−r

I. INTRODUCTION

The nature of dark matter remains one of the most significant unsolved problems in cosmology and particle physics. The abundance of dark matter has been precisely determined by observations of anisotropies in the cosmic microwave background (CMB) [1], and the measurements of the growth of cosmological structure in the clustering of galaxies [2] and in the Lyman-α forest [3]. The fundamental nature of the dark matter, however, remains unknown.

One natural candidate is a fermion that has no standard model interactions other than a coupling to the standard neutrinos through their mass generation mechanism [4,5]. Because of their lack of interactions and association with the neutrino sector, such fermions are referred to as sterile neutrinos. Observations are consistent with sterile neutrinos as the dark matter for a narrow mass range for the standard production mechanism. In this allowed range of masses, the sterile neutrino has a non-negligible thermal velocity component, and is therefore a warm dark matter (WDM) candidate.

The prevalent ansatz of an absolute cold dark matter (CDM) component in galaxy formation is not strictly valid even for one of the most cited CDM candidates, the lightest supersymmetric particle, which has a small but nonzero velocity dispersion [6,7]. The damping scale at which thermal velocities of the dark matter cut off the growth of gravitationally bound structures remains an open question. One principal challenge to the CDM paradigm is the order of magnitude overprediction of the observed satellites in galaxy-sized halos such as the Milky Way [8–11]. Warm dark matter suppresses dwarf galaxy formation, which may occur through fragmentation of larger structures [12]. Semianalytic galaxy formation modeling has found that the number of dwarf galaxies formed in satellite halos may be suppressed due to the reionization, stellar feedback within halos, and/or tidal stripping of satellites [13–17]. Such semianalytic modeling is both powerful and malleable, and must be verified in robust hydrodynamic simulations of galaxy formation. Whether a minor or major suppression of small mass halos is beneficial or detrimental to the suppression of dwarf galaxy formation remains unsolved.

Four more problems in the CDM paradigm may benefit from the reduction of power on small scales from WDM. First is the reduction of the prevalence of halos in low-density voids in N-body simulations of CDM structure formation, and consistent with the apparent dearth of massive galaxies within voids in local galaxy surveys [12,18]. The second is the relatively low concentrations of galaxies observed in rotation curves compared to what is predicted from the ΛCDM power spectrum [19,20], which can be relieved by a reduction of the initial power spectrum of density fluctuations at small scales [21,22]. The third is the ''angular-momentum'' problem of CDM halos, where gas cools at very early times into small mass halos and leads to massive low-angular momentum gas cores in galaxies, which can be alleviated by the hindrance of gas collapse and angular-momentum loss through the delay of small halo formation in a WDM scenario [23]. The fourth problem is the formation of disk-dominated or pure-disk galaxies in CDM models, which is impeded by bulge formation due to the high merger accretion rate history in CDM models, but may be alleviated with WDM [24,25].

Sterile neutrinos arise naturally in most extensions to the standard model of particle physics. Singlet neutrinos with masses relevant to oscillation experiments and dark matter can arise in grand unified models [26], string-inspired models [27], and models with large extra dimensions [28,29]. In reverence to Occam's razor, the minimalist model of Ref. [30] produces the neutrino-oscillation inferred neutrino mass hierarchy, the dark matter via a sterile

neutrino, as well as the observed baryon asymmetry in a neutrino minimal standard model (νMSM) that introduces Majorana and Dirac neutrino mass terms to the standard model Lagrangian. There is also an indication that one or more light sterile mass eigenstates may cause the flavor transformation seen in the Los Alamos Liquid Scintillator Neutrino Detector (LSND) experiment [31,32]. Another intriguing motivation for the presence of a dark matter sterile neutrino is the abundance of anomalously high pulsar velocities that may be difficult to produce in the convective hydrodyamics in a supernova, but may be produced in asymmetric sterile neutrino emission from a hot nascent neutron star [33–35]. However, whether convective overturn and the resulting global asymmetry in the ejecta alone can power the observed distribution of pulsar velocities remains an open question [36,37].

The potentially beneficial effects of the suppression of the cosmological small-scale structure in WDM can also lead to observational conflicts if the suppression extends to excessively high mass and length scales. As I shall show in detail below, the suppression scale monotonically decreases with increasing sterile neutrino particle mass. The reionization of the Universe by a redshift of $z \sim 6$ requires sufficient structure formation at very early times, and can place one of the most stringent lower bounds on the sterile neutrino mass [38,39]. The radiative decay of the sterile neutrino dark matter may, however, increase the hydrogen ionization fraction, augmenting molecular hydrogen formation, gas cooling, star formation, and therefore reionization [40]. One of the best direct measures of clustering at small scales is the clustering observed in intervening gas along the line of sight to a quasar, known as the Lyman-α forest [41]. Statistically consistent constraints allowing freedom in all cosmological parameters and constraints from the cosmic microwave background, galaxy clustering, and a measurement of clustering in the Lyman-α forest give a lower limit for the sterile neutrino dark matter particle mass as $m_s > 1.7$ keV (95% C.L.)[42].

In all studies of the types discussed above of galaxy formation, cosmological reionization, and clustering in the Lyman-α forest, robust conclusions require an accurate initial description of the fluctuations arising from the early universe. In Sec. II, I outline the production mechanism of sterile neutrino dark matter through the varying particle population in the early universe and the QCD transition, and describe the resulting nonthermal sterile neutrino energy distribution. In Sec. III, I follow the evolution of the nonthermal sterile neutrino dark matter perturbations through the radiation dominated era into the linear regime of the matter dominated era. This is related to the CDM perturbation spectrum through a transfer function. My results differ significantly from previous work on the sterile neutrino dark matter perturbation evolution [43,44] which neglected the effects of the changing particle population in the early universe, the QCD transition, and the dilution of the dark matter due to annihilation.

The sterile neutrino particle dark matter candidate studied here may be embedded in several extensions beyond the standard model of particle physics, as a superpartner, or it may have properties that would have it couple to other species at higher temperatures, including the inflaton. However, knowing its behavior in the early universe in such extensions would involve introducing a much more model dependent interaction and production mechanism, as well as knowledge of all of the degrees of freedom that are present and may annihilate and dilute the sterile neutrino in such a model between the coupling epoch and today. Even in such models with higher energy scale couplings, dilution may render the abundance of sterile neutrinos negligible upon entering the production epoch considered here of $T < 300$ MeV. The production mechanism studied here is a minimalist extension to the standard model through the neutrino mass generation mechanism, and does not require what would be at this point speculation of higher energy physics. Therefore, the initial abundance of sterile neutrinos entering the oscillation-production epoch is taken here to be nil.

II. PRODUCTION

Sterile neutrinos of interest for dark matter are never coupled to the primordial plasma. The production of sterile neutrinos in the early universe within the mass range of interest for warm to cold dark matter occurs at temperatures where collisions dominate the evolution of the neutrino system, and matter-effected oscillations are suppressed by induced thermal masses and the quantum Zeno effect. The true time evolution of the system is described by that of the density matrix [45]. However, the collision dominated regime allows a simplification of the density matrix evolution to a quasiclassical Boltzmann equation of the form [46]

$$\frac{\partial}{\partial t} f_s(p,t) - Hp \frac{\partial}{\partial p} f_s(p,t) \approx \frac{1}{4} \frac{\Gamma_\alpha(p) \Delta^2(p) \sin^2 2\theta}{\Delta^2(p) \sin^2 2\theta + D^2(p) + [\Delta(p) \cos 2\theta - V^L - V^T(p)]^2} [f_\alpha(p,t) - f_s(p,t)], \quad (1)$$

with a corresponding evolution equation for the antineutrino distributions. Here, $f_s(p,t)$ and $f_\alpha(p,t)$ are the active and sterile neutrino distribution functions, as a function of momentum, p, and time, t; $H = \dot{a}/a$ is the Hubble expansion for scale factor a; $\Delta(p) = \delta m^2/2p$ is the vacuum oscillation factor dependent on the mass-squared difference $\delta m^2 = m_s^2 - m_\alpha^2$ between the active and sterile neutrinos; the mixing angle between the two flavor states is θ.

The production is driven by the collision rate

$$\Gamma_\alpha(p) \approx \begin{cases} 1.27 G_{\rm F}^2 p T^4, & \alpha = e, \\ 0.92 G_{\rm F}^2 p T^4, & \alpha = \mu, \tau, \end{cases} \quad (2)$$

and is augmented at temperatures, T, above the quark-hadron (QCD) transition, where quarks and the massive leptons μ and τ contribute [46], and are included in the calculation here. The system is damped by the quantum Zeno effect, $D(p) = \Gamma_\alpha(p)/2$, and mixing is suppressed by the thermal potential [47]

$$V^T(p) = -\frac{8\sqrt{2} G_{\rm F} p}{3 m_{\rm Z}^2} (\langle E_{\nu_\alpha} \rangle n_{\nu_\alpha} + \langle E_{\bar{\nu}_\alpha} \rangle n_{\bar{\nu}_\alpha}) - \frac{8\sqrt{2} G_{\rm F} p}{3 m_{\rm W}^2} (\langle E_\alpha \rangle n_\alpha + \langle E_{\bar{\alpha}} \rangle n_{\bar{\alpha}}), \quad (3)$$

which has contributions from thermally populated leptons of the same flavor as the active neutrino.

The asymmetric lepton potential for flavor α is

$$V^L = \sqrt{2} G_{\rm F} \left[2(n_{\nu_\alpha} - n_{\bar{\nu}_\alpha}) + \sum_{\beta \neq \alpha} (n_{\nu_\beta} - n_{\bar{\nu}_\beta}) - \frac{n_n}{2} \right]. \quad (4)$$

Here, I will consider only lepton number symmetric universes; however, the limits on the lepton asymmetry allow for a non-negligible lepton number [48–50] which can drive resonant sterile neutrino dark matter production [5,46]. One can neglect the asymmetric potential due to the baryon number n_n, which is subdominant at all temperature scales of interest for sterile neutrino dark matter production. The temperature of peak production is approximately

$$T_{\rm peak} \approx 130 \text{ MeV} \left(\frac{m_s}{3 \text{ keV}} \right)^{1/3}. \quad (5)$$

The time evolution of the temperature-dependent thermal potential and collision rate needed to integrate the production Boltzmann equation requires knowing the time-temperature relation, and therefore the evolution of the background plasma. Details of the general time-temperature relation are given in the appendix of Ref. [46], and are summarized here. The time-temperature relation depends on the expansion-dependent change of the temperature

$$\frac{da}{dT} = \frac{d\rho_{\rm tot}}{dT} (\rho_{\rm tot} + p_{\rm tot})^{-1}, \quad (6)$$

and the Friedmann equation governing the expansion rate, $da/dt = 3H$. The standard evolutions of the pressure and temperature are affected by the changing thermal population of particle species, which I calculate using the known standard model particle mass distribution [51].

A critical consideration for dark matter production is the fact that production occurs near the temperature of the quark-hadron transition [52]. Lattice QCD calculations of two massless u, d quarks and an infinitely massive s quark show a crossover type transition at $T_{\rm QCD} = 173 \pm 8$ MeV [53]; more realistic $(2 + 1)$ quark flavor lattice calculations find a transition at $T_{\rm QCD} = 169 \pm 12(\text{stat}) \pm 4(\text{syst})$ MeV [54]. Overall, due to hadron and lepton population as well as the quark-hadron transition, the statistical degrees of freedom of the plasma, g_*, change by nearly an order of magnitude in the temperature range of interest for sterile neutrino dark matter production. In addition, the annihilation of these species heats the coupled plasma relative to the (constantly) decoupled sterile neutrinos, which are subsequently diluted and spectrally distorted. Note that production is also affected by the temperature range of the softness of the crossover transition. Motivated by Ref. [54], I model the softness of the crossover as rapid, over 5 MeV at $T_{\rm QCD} = 170$ MeV. Changes to the softness of the transition affect the production abundance by only a few percent.

For low-mass sterile neutrinos, $m_s < 0.5$ keV, production occurs at low temperatures where the statistical degrees of freedom in the primordial plasma are changing minimally, and one may set g_* to be constant so that the production Eq. (1) can be integrated analytically [4]. In this approximation, the momentum dependence of the production disappears, and the sterile neutrino momentum distribution is simply a suppressed active neutrino distribution.

However, for $m_s \gtrsim 0.5$ keV, in order to accurately include the strong changes in the plasma background, the quark-hadron transition, dark matter dilution, the modification of scattering rates, and flavor-dependent modification of the thermal potential [Eq. (3)], the production equation must be integrated numerically, and the result is momentum dependent. In order to test the accuracy of the numerical calculation, I solve the analytically solvable case of a simple power-law time-temperature relation as well as all of the other simplifications of the analytic case, but with the full momentum distribution of neutrinos. The numerical integration recovers the analytic result within 1%. In Fig. 1, I show the resulting relative distribution of sterile to active neutrinos $\rho(\epsilon) = f_s(\epsilon)/f_\alpha(\epsilon)$ for masses in the range $0.3 < m_s < 140$ keV, with $\epsilon \equiv p/T$. Note that all cases are distorted from a pure constant suppression, and are increasingly distorted for more massive neutrinos, which are produced at higher temperatures [Eq. (5)] where the effects described above are more pronounced. One of the dominant effects is the cooling and subsequent enhancement of the low momentum sterile neutrino distribution due to the heating of the plasma, including the active neutrinos, from particle annihilations. Another feature is the enhancement at $\epsilon < 1$ for lower-mass neutrinos due to the production of these momenta during the slow temporal evolution of the temperature through the quark-hadron transition.

The work on sterile neutrino dark matter production of Ref. [55] follows that of Ref. [4] except for an extension to

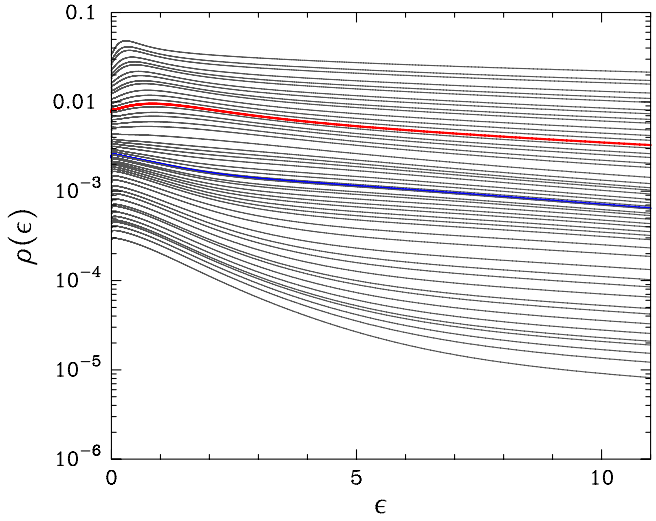

FIG. 1 (color online). The resulting relative distribution coming from the production epoch for sterile neutrino dark matter relative to the active neutrinos, $\rho(\epsilon) = f_s(\epsilon)/f_\alpha(\epsilon)$, $(\epsilon \equiv p/T)$ over a mass range $0.3 < m_s < 140$ keV, for 50 cases, and increasing m_s having decreasing distribution amplitudes. All cases have $\Omega_{\rm DM} = 0.26$. The upper thick (red) line is for the case of $m_s = 1.7$ keV and the lower thick (blue) line is for the case $m_s = 8.2$ keV.

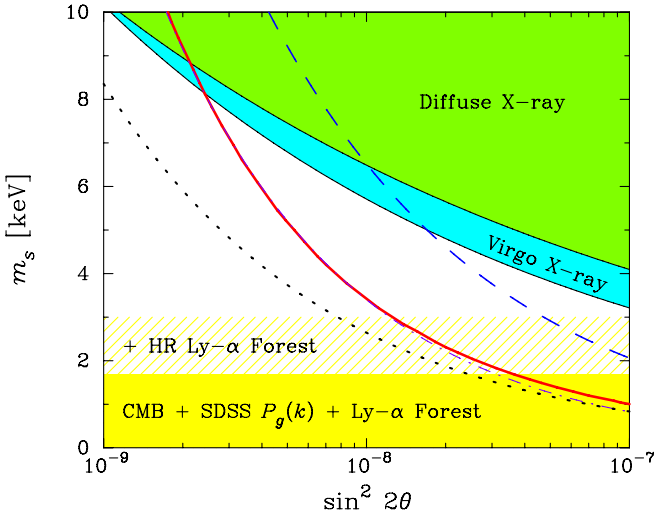

FIG. 2 (color online). Contours of predicted critical density $\Omega_{\rm DM} = 0.26$ from the direct numerical calculation in this work (solid red curve), the fit provided here (dot-dashed purple curve), the results of Ref. [46] which used a different quark-hadron transition and particle population model (dashed blue curve), and that of Ref. [55] (dotted black curve) for the inaccurate but common choice of $g'_* = 10.75$ (more realistic choices of g'_* make the predicted abundance more inaccurate). Also shown are the upper flux constraint from x-ray observations of the Virgo cluster [56], the constraint from the diffuse x-ray background [57], the lower-mass constraint from the CMB, SDSS galaxy clustering and Lyman-α forest, and the possible constraint from also including the high-resolution (HR) Lyman-α forest [42].

$m_s > 0.5$ keV via the inclusion of an unknown factor $(g'_*/10.75)$ within the production "prediction" relationship, with an effective production statistical degree of freedom, g'_*. The resulting relation lacked predictivity due to the power-law dependence on an unknown g'_*. The major effect of the high degrees of freedom at the production temperatures is dilution of the sterile neutrinos, so that the production dependence on an increased g'_* is an inverse relation. The sign and value of the dependency on g'_* in the production prediction equation of Ref. [55] was noted in Ref. [43] as a typographical error. Using the common but incorrect choice of $g'_* = 10.75$, the production relation in Ref. [55] is inaccurate, as shown in Fig. 2.

In Fig. 2, I show the contours of critical density in sterile neutrino dark matter density for varying mass and mixing for an electron neutrino flavor mixed with the sterile neutrino. I also show the results of Ref. [55] for the common choice of $g'_* = 10.75$, which is inaccurate, but choices of a more realistic effective production temperature g'_* increase the discrepancy. I also show the results of Ref. [46], which used $T_{\rm QCD} = 100$ MeV and a different model of the hadron and lepton population distributions based on an older catalog of particle masses. The critical density contour of Ref. [46] lies at higher mixing angles because an increased coupling was required to offset the dilution of the QCD transition set at $T_{\rm QCD} = 100$ MeV, which occurs below the bulk of production of all sterile neutrino masses $m_s \gtrsim 1$ keV. The full numerical results for the predicted dark matter abundance from this work are fit well by the relation

$$m_s = 3.40\ \text{keV}\left(\frac{\sin^2 2\theta}{10^{-8}}\right)^{-0.615}\left(\frac{\Omega_{\rm DM}}{0.26}\right)^{0.5} \times \left\{0.527\ \text{erfc}\left[-1.15\left(\frac{T_{\rm QCD}}{170\ \text{MeV}}\right)^{2.15}\right]\right\}, \quad (7)$$

for an electron neutrino flavor mixed with the sterile neutrino. This expression is valid for $135 < T_{\rm QCD} < 300$ MeV. Note that the quantity within curled brackets is unity for $T_{\rm QCD} = 170$ MeV.

This new relationship between the critical density fraction, m_s and $\sin^2 2\theta$ modifies the flux constraint observed from the Virgo cluster [56], so that the inferred upper bound on the mass of the sterile neutrino dark matter is now

$$m_s < 8.2\ \text{keV}. \quad (8)$$

This is the result of the fact that the constraint in Ref. [56] is not a direct mass constraint but a flux constraint, which is related to the radiative decay rate through the mass-mixing angle relation. Lines of constant flux follow the fourth power of the mass since the decay rate increases as the fifth power, but the number density in the field of view decreases proportionally with the mass. Using the production relationship, Eq. (7), the diffuse x-ray background limit of Ref. [57] is

$$m_s < 8.89 \text{ keV} \left(\frac{\Omega_{\rm DM}}{0.26}\right)^{0.538}, \quad (9)$$

for central values of the cosmological parameters, and is shown in Fig. 2. The constraints from unresolved x-ray sources derived by Mapelli and Ferrara [58] are similar to Eq. (9), when using the production relation Eq. (7) [59].

III. PERTURBATION EVOLUTION

The standard cosmological model of structure formation from adiabatic Gaussian fluctuations seeded by an inflationary epoch is affected by perturbation growth in the radiation through matter dominated eras. The distribution of velocities of the dark matter suppresses fluctuations below its free streaming scale, which increases with the mean dark matter velocities and decreases with its mass. Since sterile neutrinos are produced nonthermally, their full energy distribution must be included in an accurate calculation of the fluctuation spectrum arising from the linear growth epoch. I use the approach of the covariant multipole perturbation evolution equations for massive neutrinos in Ref. [60] and implemented in the Code for Anisotropies in the Microwave Background (CAMB) [61]. The multipole equations depend on the value of the massive neutrino energy distribution and its momentum derivative, but I will not reproduce them here.

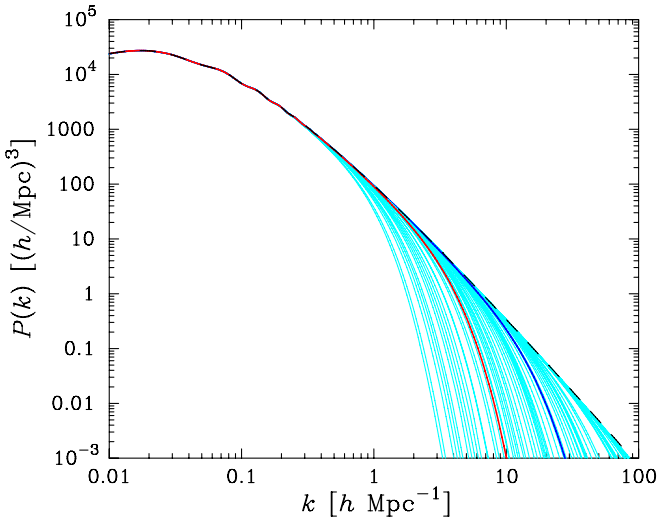

FIG. 3 (color online). Shown are the resulting linear matter power spectra for nonthermal sterile neutrinos in the mass range $0.3 < m_s < 140$ keV (gray/cyan). The thick (red) low-k suppression case is for the lower-mass limit inferred from the Lyman-α forest ($m_s > 1.7$ keV), and the thick (blue) high-k suppression case is for the upper-mass limit from x-ray observations of the Virgo cluster ($m_s < 8.2$ keV). The CDM case is the dashed (black) line. Measures of large-scale structure in the linear regime are in the region of $0.01h < k < 0.2h$ Mpc^{-1} for galaxy surveys, while neutral gas clustering observed in the Ly-α forest may extend observations of linear structure to $0.1h < k < 3h$ Mpc^{-1}.

I calculate the growth of perturbations through the radiation and matter dominated epochs of sterile neutrino dark matter with CAMB. I include directly the numerically calculated momentum-dependent sterile neutrino distribution functions and their derivatives from the solution of the quasiclassical Boltzmann Eq. (1) as described in the previous section. The resulting linear matter power spectra today at redshift zero are shown in Fig. 3 for a range of sterile neutrino masses from 0.3 to 140 keV, along with the related CDM case.

A useful form of the suppressed perturbation power spectrum $P_{\rm sterile}(k)$ relative to the CDM case is a sterile neutrino transfer function of the form

$$T_s(k) \equiv \sqrt{\frac{P_{\rm sterile}(k)}{P_{\rm CDM}(k)}}, \quad (10)$$

which can be used to convert any CDM transfer function to that of sterile neutrino dark matter. I find a fitting function that describes the transfer function of the form

$$T_s(k) = [1 + (\alpha k)^\nu]^{-\mu}, \quad (11)$$

where

$$\alpha = a\left(\frac{m_s}{1 \text{ keV}}\right)^b \left(\frac{\Omega_{\rm DM}}{0.26}\right)^c \left(\frac{h}{0.7}\right)^d h^{-1} \text{ Mpc}, \quad (12)$$

and $a = 0.189$, $b = -0.858$, $c = -0.136$, $d = 0.692$, $\nu = 2.25$, and $\mu = 3.08$. The fitting form is valid for $0.3 \lesssim m_s \lesssim 15$ keV. This fitting function is shown relative to our numerical results in Fig. 4 as well as previous results by Ref. [43]. Note that all of the features of the numerical

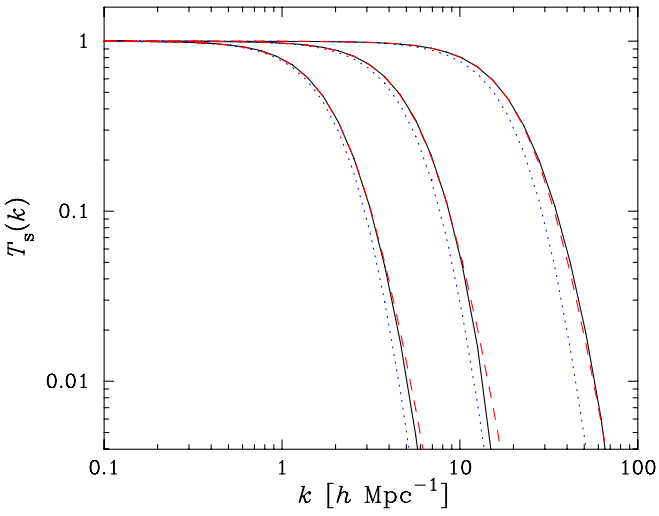

FIG. 4 (color online). Shown here is the relative sterile neutrino transfer function $T_s(k)$ to CDM for the same large-scale amplitude of perturbations, for the cases of $m_s = 0.5$, 1.7, 8.2 keV with increasing wave number k suppression scale, respectively. The solid (black) lines are from the full numerical calculation, the dashed (red) lines are the fitting form in Eq. (11), and the dotted (blue) lines are the results of Ref. [43].

results are not obtained in the fit due to the nonthermal character of the sterile neutrino distribution, particularly for $m_s = 1.7$ keV where peak production occurs near the quark-hadron transition.

The result presented here for the relative sterile neutrino transfer function is similar, yet significantly different from previous work [43,44], with the difference attributed to the use here of the nonthermal sterile neutrino momentum distribution due to the physics described in Sec. II. The results derived here differ in cosmological parameter dependence of $T_s(k)$ from 2% to 18% and in the rapidity of the cutoff μ at 45% relative to that in Refs. [43,44]. Using the transfer function derived here and small-scale clustering data sets including the inferred matter power spectrum from the high-resolution Lyman-α forest from Viel *et al.* [62], Ref. [42] found lower limits on the mass of the sterile neutrino dark matter at 1.7 keV (95% C.L.) from the CMB, the SDSS 3D $P_g(k)$ of galaxies [63] plus SDSS Lyman-α forest [64], and a lower limit of 3.0 keV (95% C.L.) if the inferred matter power spectrum from the high-resolution Lyman-α forest of Ref. [62] is used, which however has significant systematic uncertainties.

IV. CONCLUSIONS

Potential problems in galaxy and small-scale structure formation indicate the possibility of a small-scale velocity damping of perturbations of the type in warm dark matter such as sterile neutrino dark matter. Here, I have presented the calculation of the production and linear perturbation evolution in the early universe of sterile neutrino dark matter. Included were the essential effects of the change in Friedmann dynamics dictated by the quark-hadron transition and particle population, the alteration of finite temperature effective mass of active neutrinos due to the presence of thermal leptons, and heating of the coupled species due to the disappearance of degrees of freedom in the plasma. The resulting sterile neutrinos have a nontrivial momentum distribution that is grossly nonthermal.

Using the resulting energy distributions of sterile neutrinos, I have calculated the evolution of sterile neutrino density perturbations in the early universe through the linear regime and provide a fitting function form for the transfer function describing the suppression of small-scale fluctuations for this warm dark matter candidate. The results presented here differ significantly from previous work due to the inclusion of relevant physical effects.

The results of the linear perturbation evolution presented here are necessary as initial conditions for addressing the questions of structure formation and galaxy formation in the case of a sterile neutrino dark matter candidate with a nontrivial velocity distribution. Following structure formation in this case into the nonlinear regime will allow a resolution of the question of whether observations of galactic structure at small scales are indicating a method of inferring the properties and—ultimately—the identity of the dark matter.

ACKNOWLEDGMENTS

I thank Antony Lewis for assistance with CAMB, Gerard Jungman for help with the rational function fitting forms, Tanmoy Bhattacharya and Rajan Gupta for useful discussions regarding lattice methods in studies of the quark-hadron transition, and Salman Habib and Julien Lesgourgues for very useful comments on the manuscript. This work was supported by Los Alamos National Laboratory under DOE Contract No. W-7405-ENG-36.

[1] D. N. Spergel *et al.* (WMAP Collaboration), Astrophys. J. Suppl. Ser. **148**, 175 (2003).
[2] M. Tegmark *et al.* (SDSS Collaboration), Phys. Rev. D **69**, 103501 (2004).
[3] U. Seljak *et al.*, Phys. Rev. D **71**, 103515 (2005).
[4] S. Dodelson and L. M. Widrow, Phys. Rev. Lett. **72**, 17 (1994).
[5] X.-d. Shi and G. M. Fuller, Phys. Rev. Lett. **82**, 2832 (1999).
[6] S. Hofmann, D. J. Schwarz, and H. Stoecker, Phys. Rev. D **64**, 083507 (2001).
[7] G. Jungman, M. Kamionkowski, and K. Griest, Phys. Rep. **267**, 195 (1996).
[8] G. Kauffmann, S. D. M. White, and B. Guiderdoni, Mon. Not. R. Astron. Soc. **264**, 201 (1993).
[9] A. A. Klypin, A. V. Kravtsov, O. Valenzuela, and F. Prada, Astrophys. J. **522**, 82 (1999).
[10] B. Moore *et al.*, Astrophys. J. **524**, L19 (1999).
[11] B. Willman, F. Governato, J. Wadsley, and T. Quinn, Mon. Not. R. Astron. Soc. **353**, 639 (2004).
[12] P. Bode, J. P. Ostriker, and N. Turok, Astrophys. J. **556**, 93 (2001).
[13] A. Dekel and J. Silk, Astrophys. J. **303**, 39 (1986).
[14] A. A. Thoul and D. H. Weinberg, Astrophys. J. **465**, 608 (1996).
[15] J. S. Bullock, A. V. Kravtsov, and D. H. Weinberg, Astrophys. J. **548**, 33 (2001).
[16] J. S. Bullock, A. V. Kravtsov, and D. H. Weinberg, Astrophys. J. **539**, 517 (2000).
[17] A. J. Benson, C. G. Lacey, C. M. Baugh, S. Cole, and C. S. Frenk, Mon. Not. R. Astron. Soc. **333**, 156 (2002).
[18] P. J. E. Peebles, astro-ph/0101127.
[19] J. J. Dalcanton and C. J. Hogan, Astrophys. J. **561**, 35 (2001).
[20] F. C. van den Bosch and R. A. Swaters, Mon. Not. R.

Astron. Soc. **325**, 1017 (2001).
[21] A. R. Zentner and J. S. Bullock, Phys. Rev. D **66**, 043003 (2002).
[22] K. Abazajian, S. M. Koushiappas, and A. R. Zentner (to be published).
[23] A. D. Dolgov and J. Sommer-Larsen, Astrophys. J. **551**, 608 (2001).
[24] F. Governato *et al.*, Astrophys. J. **607**, 688 (2004).
[25] J. Kormendy and D. B. Fisher, Rev. Mex. Astron. Astrofis. (Serie de Conferencias) **23**, 101 (2005).
[26] B. Brahmachari and R. N. Mohapatra, Phys. Lett. B **437**, 100 (1998).
[27] P. Langacker, Phys. Rev. D **58**, 093017 (1998).
[28] G. R. Dvali and A. Y. Smirnov, Nucl. Phys. **B563**, 63 (1999).
[29] K. Abazajian, G. M. Fuller, and M. Patel, Phys. Rev. Lett. **90**, 061301 (2003).
[30] T. Asaka, S. Blanchet, and M. Shaposhnikov, Phys. Lett. B **631**, 151 (2005).
[31] C. Athanassopoulos *et al.* (LSND Collaboration), Phys. Rev. Lett. **81**, 1774 (1998).
[32] M. Sorel, J. M. Conrad, and M. Shaevitz, Phys. Rev. D **70**, 073004 (2004).
[33] A. Kusenko and G. Segre, Phys. Rev. D **59**, 061302 (1999).
[34] G. M. Fuller, A. Kusenko, I. Mocioiu, and S. Pascoli, Phys. Rev. D **68**, 103002 (2003).
[35] A. Kusenko, Int. J. Mod. Phys. D **13**, 2065 (2004).
[36] L. Scheck, T. Plewa, H.-T. Janka, K. Kifonidis, and E. Mueller, Phys. Rev. Lett. **92**, 011103 (2004).
[37] C. L. Fryer and A. Kusenko, astro-ph/0512033.
[38] R. Barkana, Z. Haiman, and J. P. Ostriker, Astrophys. J. **558**, 482 (2001).
[39] N. Yoshida, A. Sokasian, L. Hernquist, and V. Springel, Astrophys. J. **591**, L1 (2003).
[40] P. L. Biermann and A. Kusenko, astro-ph/0601004 [Phys. Rev. Lett. (to be published)].
[41] V. K. Narayanan, D. N. Spergel, R. Dave, and C.-P. Ma, Astrophys. J. **543**, L103 (2000).
[42] K. Abazajian, astro-ph/0512631 [Phys. Rev. D (to be published)].
[43] M. Viel, J. Lesgourgues, M. G. Haehnelt, S. Matarrese, and A. Riotto, Phys. Rev. D **71**, 063534 (2005).
[44] S. H. Hansen, J. Lesgourgues, S. Pastor, and J. Silk, Mon. Not. R. Astron. Soc. **333**, 544 (2002).
[45] B. H. J. McKellar and M. J. Thomson, Phys. Rev. D **49**, 2710 (1994).
[46] K. Abazajian, G. M. Fuller, and M. Patel, Phys. Rev. D **64**, 023501 (2001).
[47] D. Notzold and G. Raffelt, Nucl. Phys. **B307**, 924 (1988).
[48] A. D. Dolgov *et al.*, Nucl. Phys. **B632**, 363 (2002).
[49] K. N. Abazajian, J. F. Beacom, and N. F. Bell, Phys. Rev. D **66**, 013008 (2002).
[50] Y. Y. Y. Wong, Phys. Rev. D **66**, 025015 (2002).
[51] S. Eidelman *et al.*, Phys. Lett. B **592**, 1 (2004); URL http://pdg.lbl.gov
[52] K. N. Abazajian and G. M. Fuller, Phys. Rev. D **66**, 023526 (2002).
[53] F. Karsch, E. Laermann, and A. Peikert, Nucl. Phys. **B605**, 579 (2001).
[54] C. Bernard *et al.* (MILC Collaboration), Phys. Rev. D **71**, 034504 (2005).
[55] A. D. Dolgov and S. H. Hansen, Astropart. Phys. **16**, 339 (2002).
[56] K. Abazajian, G. M. Fuller, and W. H. Tucker, Astrophys. J. **562**, 593 (2001).
[57] A. Boyarsky, A. Neronov, O. Ruchayskiy, and M. Shaposhnikov, astro-ph/0512509.
[58] M. Mapelli and A. Ferrara, Mon. Not. R. Astron. Soc. **364**, 2 (2005).
[59] M. Mapelli (private communication).
[60] A. Lewis and A. Challinor, Phys. Rev. D **66**, 023531 (2002).
[61] A. Lewis, A. Challinor, and A. Lasenby, Astrophys. J. **538**, 473 (2000), URL http://camb.info.
[62] M. Viel, M. G. Haehnelt, and V. Springel, Mon. Not. R. Astron. Soc. **354**, 684 (2004).
[63] M. Tegmark *et al.* (SDSS Collaboration), Astrophys. J. **606**, 702 (2004).
[64] P. McDonald *et al.*, Astrophys. J. **635**, 761 (2005).